

# RNA-seq analyses of antibiotic resistance mechanisms in *Serratia marcescens*

ZHAODONG LI<sup>1</sup>, MEIHUA XU<sup>1</sup>, HUI WEI<sup>1</sup>, LILI WANG<sup>1</sup> and MIN DENG<sup>2</sup>

<sup>1</sup>Clinical Laboratory; <sup>2</sup>Emergency Department, Hangzhou Red Cross Hospital, Hangzhou, Zhejiang 310004, P.R. China

Received August 3, 2018; Accepted February 28, 2019

DOI: 10.3892/mmr.2019.10281

**Abstract.** The present study aimed to further clarify the genetic mechanisms responsible for the antimicrobial resistance of *Serratia marcescens* (*S. marcescens*) using RNA sequencing. Three drug-susceptible *S. marcescens* strains (named MYQT1, MYQT2, and MYQT3) and three multidrug-resistant *S. marcescens* strains (named MYQT4, MYQT5, and MYQT6) were isolated from six different patients and subjected to RNA sequencing. Differentially expressed genes (DEGs) between the multidrug-resistant *S. marcescens* strains and drug-susceptible strains were screened and compared, followed by functional enrichment analysis. In addition, a protein-protein interaction (PPI) network was constructed, and significant modules were extracted from it. Genes enriched in the significant modules were subjected to further enrichment analysis. MYQT3 had very a different expression pattern from MYQT1 and MYQT2, and thus, MYQT3 was excluded from the following analysis. A total of 225 DEGs were identified, of which SMDB11\_RS09300 (GTP cyclohydrolase Fole2) was the most significantly upregulated with a log<sub>2</sub> FC of 6.4; these DEGs were enriched in different GO terms, including hydrogen sulfide biosynthetic process, sulfur compound transmembrane transporter activity, and ABC transporter complex. Additionally, several genes were identified to be important genes in the PPI network, including SMDB11\_RS17755 (upregulated; glutamate synthase large subunit), SMDB11\_RS00590 (upregulated; sulfite reductase subunit  $\alpha$ ), and SMDB11\_RS04505 (upregulated; cystathionine

$\beta$ -synthase). Thus, SMDB11\_RS09300, SMDB11\_RS17755, SMDB11\_RS00590, and SMDB11\_RS04505 may play significant roles in the antimicrobial resistance of *S. marcescens* by participating in folate metabolism or the integrity of cell membranes. However, further experiments are required to clarify these findings.

## Introduction

Multidrug-resistant bacterial infections, especially those caused by Gram-negative pathogens, have become a significant global public health threat, and they result in considerable patient mortality and morbidity and cause great economic and production losses in the community (1). *Serratia marcescens* (*S. marcescens*), a Gram-negative bacillus, is an important nosocomial pathogen that can cause an array of infections, such as bloodstream infections, pneumonia, urinary tract infections, central nervous system infections, and conjunctivitis (2). The development of novel antibiotics, especially those used to treat multidrug-resistant pathogens, has stagnated over the last half century. Therefore, gaining more insights into the genetic mechanisms responsible for the antimicrobial resistance of pathogens is both urgent and necessary.

The accumulation of evidence has led to the identification of a number of genes that are responsible for intrinsic resistance to different classes of antibiotics, including  $\beta$ -lactams, aminoglycosides, and fluoroquinolones (3). Intrinsic mechanisms underlying bacterial antibiotic resistance include naturally occurring genes found in the chromosome of the host, such as the multiple multidrug-resistant efflux systems of  $\beta$ -lactamase of Gram-negative bacteria (4). A recent study reported an isolate of *S. marcescens* harboring the 16S rRNA methyltransferase gene *rmtB*, together with various  $\beta$ -lactamase genes and quinolone resistance genes (5). Another study revealed that imipenem-resistance in *S. marcescens* may be mediated by the plasmid expression of *Klebsiella pneumoniae* carbapenemase-2 (KPC-2) (6). In addition, evidence has demonstrated that Gram-negative bacteria can employ several strategies to protect themselves from polymyxin antibiotics, including a variety of lipopolysaccharide (LPS) modifications in addition to the formation of capsules, use of efflux pumps, and overexpression of the outer membrane protein OprH (7). Although many studies aimed at elucidating the underlying mechanisms of antibiotic resistance have been performed, much remains

---

**Correspondence to:** Dr Min Deng, Emergency Department, Hangzhou Red Cross Hospital, 208 Huancheng East Road, Hangzhou, Zhejiang 310004, P.R. China  
E-mail: minlyd888@163.com

**Abbreviations:** KPC-2, *Klebsiella pneumoniae* carbapenemase-2; LPS, lipopolysaccharide; DEGs, differentially expressed genes; PPI, protein-protein interaction

**Key words:** *Serratia marcescens*, multidrug-resistance, differentially expressed genes, functional enrichment analysis, protein-protein interaction network

largely unknown, especially the molecular mechanisms of the multi-drug resistance of *S. marcescens*, and awaits discovery.

The development of next-generation sequencing technologies has provided valuable resources for genetic research and other scientific disciplines (8,9). In this study, the parental *S. marcescens* strain and *S. marcescens* strains exhibiting multidrug-resistance were analyzed with high-throughput RNA sequencing to identify variations at the transcriptome level. Differentially expressed genes (DEGs) between the parental strain and the multidrug-resistant *S. marcescens* strains were screened, followed by functional enrichment analysis, protein-protein interaction (PPI) network construction, and module extraction. The results provide additional molecular clues that will aid in elucidating the mechanisms and metabolic pathways related to multidrug-resistance in *S. marcescens*.

## Materials and methods

**Bacterial strains and culture conditions.** Bacterial isolation, identification, and culture were performed according to conventional methods. The strains were derived from sputum, blood, lavage fluid, urine, and throat swab samples; transferred onto Columbia agar supplemented with 5% sheep blood (bioMérieux, Marcy l'Etoile, France) and MacConkey's agar plates; and incubated at 35°C for 24 h. The oxidase-negative Gram-negative bacilli was identified using the VITEK® 2 GN card (bioMérieux) (10). The drug sensitivity AST-GN16 card was used to test the antimicrobial agent susceptibility of the isolated strains. In this study, a total of three drug-susceptible *S. marcescens* strains (named MYQT1, MYQT2, and MYQT3) and three multidrug-resistant *S. marcescens* strains (named MYQT4, MYQT5, and MYQT6) were obtained from six different patients and used for the follow-up analysis.

**Total RNA extraction.** The cultures were centrifuged at 8,000 x g to precipitate bacterial cells. Total RNA was extracted using the hot phenol method as previously described with modifications (11). Subsequently, the bacterial cells were washed two times with RNase-free saline or phosphate-buffered saline (PBS; cat. no. E607016-0500; BBI solutions, Cardiff, UK). Then, 400-600 µl TES solution was added according to the precipitation amount, and the bacterial cells were resuspended. The same amount of phenol-water (Sinopharm Chemical Reagent Co., Ltd., Shanghai, China) was added followed by violent mixing. Centrifuge tubes containing a mixture of each sample, TES, and phenol-water were agitated at 65°C for 30-60 min in a Thermomixer Compact 5350 (Eppendorf, Hamburg, Germany), and then, the tubes were placed on ice and allowed to stand for 5 min. Then, the mixtures were centrifuged at 11,000 x g for 10 min at 4°C. The upper aqueous phase was selected and transferred to a new tube. Subsequently, a 1/2 volume of TRK-1002 lysis-solution and 2/3 volume of 95% ethyl alcohol was added to the upper aqueous phase, followed by vortex blending. Total RNA was then extracted using a TRK-1002 Purification kit (LC Sciences, Houston TX, USA), following the manufacturer's instructions. RNA quality was evaluated using an Agilent Bioanalyser (Agilent Technologies, Inc., Santa Clara, CA, USA).

**Library preparation and Illumina sequencing.** To remove ribosomal RNA, we used a Ribo-Zero™ Magnetic kit (Bacteria) (cat. no. MRZB12424; Illumina, Inc., San Diego, CA, USA) according to the manufacturer's protocol. RNA samples were subjected to further purification using a Zymo RNA Clean and Concentrator kit (cat. no. R1015; Zymo Research, Irvine, CA, USA) to enrich the mRNA according to the manufacturer's instructions. Each mRNA sample was suspended in 10 µl of RNase-free water, and the concentration of the obtained RNA was determined. Bacterial mRNA was fragmented and stranded, and paired-end libraries of total RNA were generated using Illumina TruSeq Stranded Total RNA HT Sample Preparation kits (cat. no. RS-122-2203, Illumina, Inc.). All the samples were sequenced using an Illumina HiSeq X10 sequencer (Illumina, Inc.).

**Mapping of reads and differential expression analysis.** RNA-seq datasets were obtained from six samples from two experiment settings. The original RNA-seq datasets were MYQT1, MYQT2, MYQT3, MYQT4, MYQT5, and MYQT6 with 9748744, 9669644, 9765080, 9638041, 9742165, and 9750956 read pairs. All RNA-seq reads were cleaned with Trimmomatic (12), and then, the read qualities were ascertained with FastQC (<https://www.bioinformatics.babraham.ac.uk/projects/fastqc/>). In order to determine the appropriate reference genome to use for read mapping, all cleaned RNA-seq reads we first used to perform BLAST (<ftp://ftp.ncbi.nlm.nih.gov/blast/executables/blast+/LATEST/>) searches against the NCBI nt database. The BLAST results indicated that *S. marcescens subsp. marcescens Db11* was the closest reference genome. The six cleaned RNA-seq datasets to *S. marcescens subsp. marcescens Db11* were then mapped using Bowtie 2 (13). In addition, the genomic viewer Integrative Genomics Viewer (IGV) (14) was used to evaluate the mapping quality. BEDtools (15) was used to calculate the read count of each gene over the six samples. Correlation analysis was performed to ensure that the read count qualities were stable within samples (across three different batches).

edgeR (16) uses the calcNormFactors function to normalize for RNA composition by finding a set of scaling factors for the library sizes that minimize the log-fold changes (FC) between the samples for most genes (16). In this study, edgeR (16) was used to perform differential gene expression analysis. edgeR uses the Cox-Reid profile-adjusted likelihood (CR) method for estimating dispersions (16). The screening criteria were  $\log_2FC > 1$  and a P-value  $< 0.05$ . Additionally, IGV was used to zoom in on some significant DEGs.

**Functional enrichment of DEGs.** The functional enrichment tool DAVID (17) was applied to perform enrichment analysis. In the analysis, functional annotations of gene ontology (GO), including the ontology of cellular component (CC), biological process (BP), and molecular function (MF) were mostly focused on (18). The GO terms with a gene count  $> 2$  and a P-value  $< 0.05$  were considered statistically significant.

**PPI construction and analysis.** The STRING database (19) contains known and predicted protein-protein associations that are integrated and transferred across organisms. Since *S. marcescens* in this study was not included in the STRING

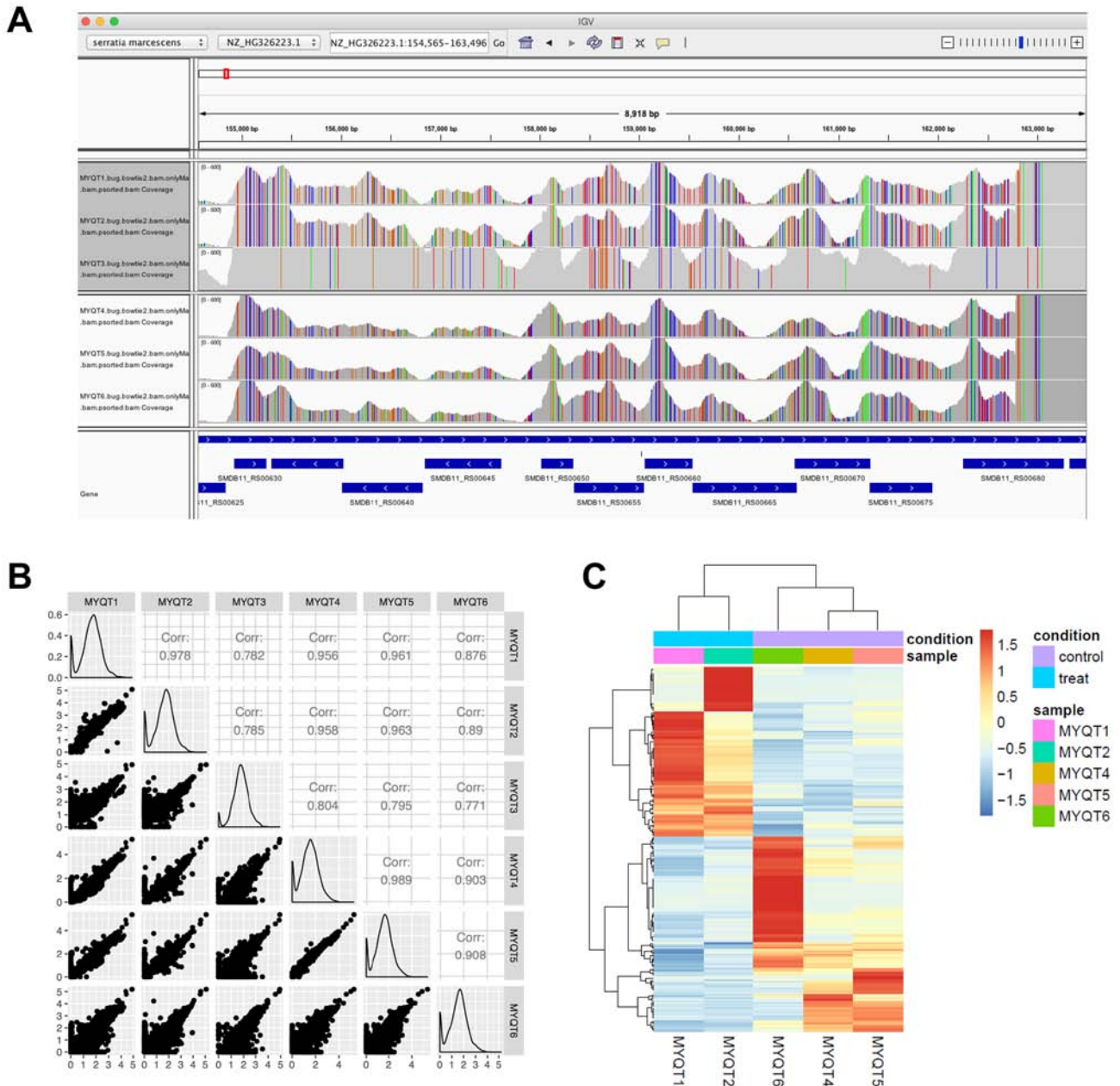


Figure 1. IGV plot, scatter plot revealing the correlation of gene expression, and heat map of DEGs. (A) IGV plot of the genomic region that corresponds to most of the samples with a high read coverage. (B) Scatter plot revealing the correlation of gene expression. (C) Heat map of DEGs. Red indicates upregulated genes, and blue indicates downregulated genes. IGV, Integrative Genomics Viewer; DEGs, differentially expressed genes.

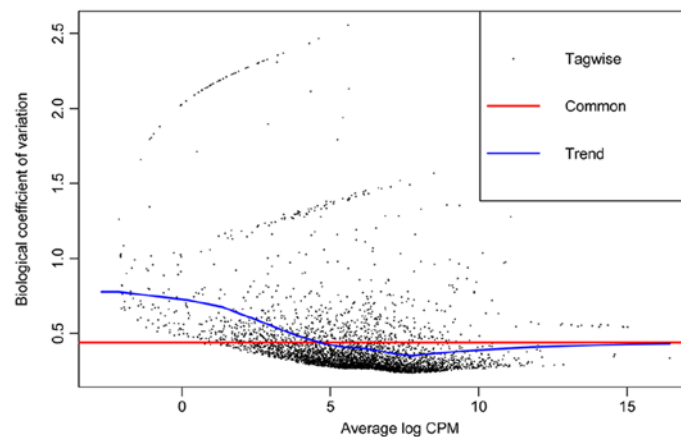


Figure 2. Dispersion plots. plotBCV illustrates the relationship of the biological coefficient of variation with the mean log counts per million.

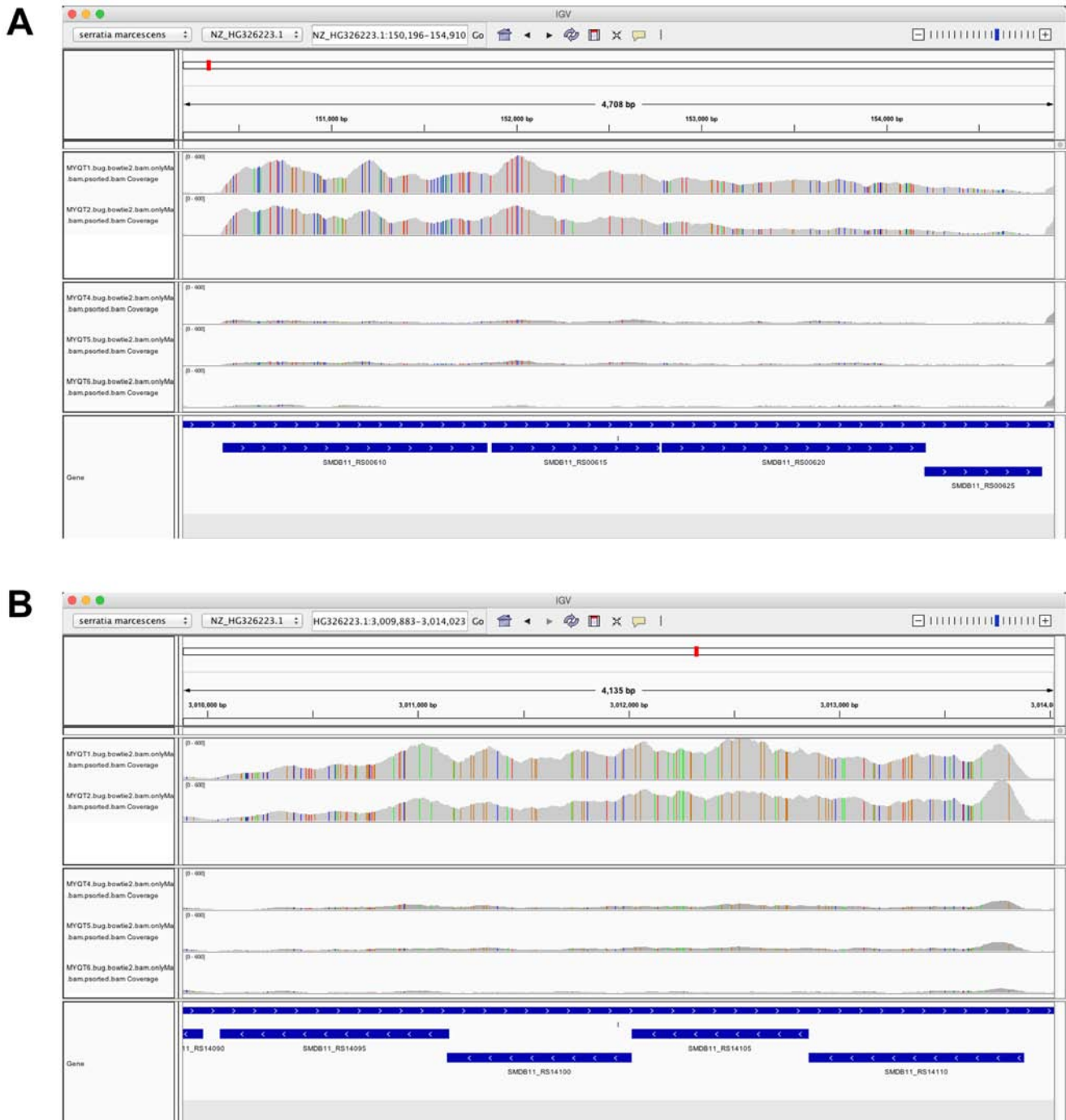


Figure 3. IGV plot of two genomic regions. (A) IGV plot of the region from locus tag SMDB11\_RS00610 to SMDB11\_RS00625. (B) IGV plot of the genomic region from locus tag SMDB11\_RS14095 to SMDB11\_RS14110. IGV, Integrative Genomics Viewer.

database, the *Serratia odorifera* 4Rx13 strain was used in the database which has a high degree of homology with *S. marcescens*. The protein sequences of the DEGs were downloaded from the NCBI database and blasted in the STRING database, and the interactions between the proteins were predicted. Required Confidence (combined score) >0.4 was selected as the threshold for predicting PPIs.

Cytoscape 3.4.0 (<https://cytoscape.org/>) is an open source software project for biological network visualization and data integration. According to the network connectivity, important nodes in the PPI network could be identified (20). In the present study, three calculation methods for determining

network topology properties were combined, including degree centrality (21), betweenness centrality (22), and closeness centrality (23), and the importance of nodes was analyzed in the network. The Cytoscape plugin CytoNCA (24) was used for the calculation of network topology properties (parameter setting: Network, without weight). In CytoNCA output, the higher the node score is, the more important the position in the network, and the more likely it is to be the key node.

**Module selection and analysis.** In PPI networks, similar functional proteins tend to cluster together and co-occur in central network locations (25). Therefore, studying the protein



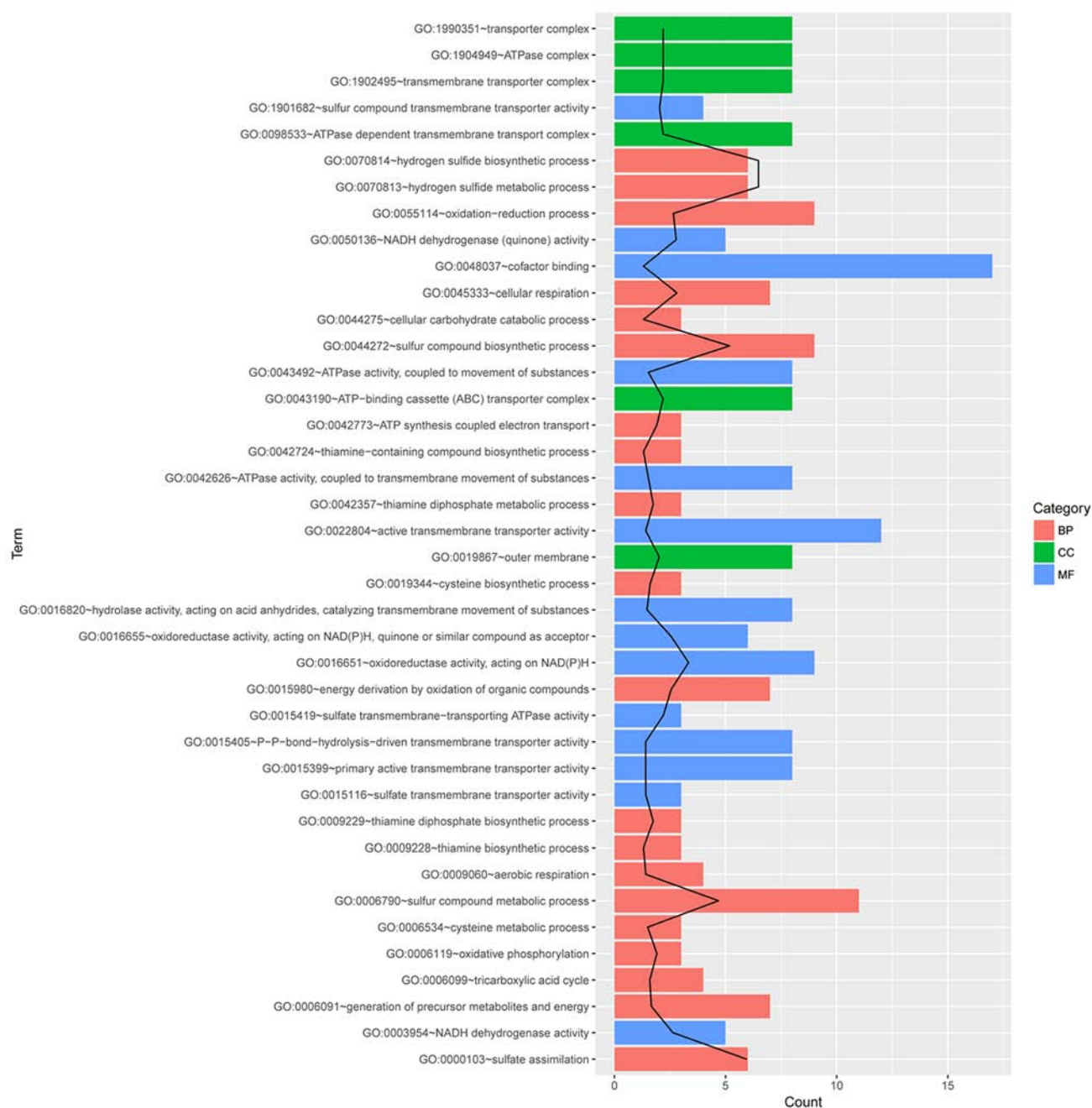


Figure 4. Functional enrichment analysis of DEGs. Count represents the number of genes enriched into a term. The black line indicates the  $-\log_{10}(P\text{-value})$ . DEGs, differentially expressed genes; CC, cellular component; BP, biological process; MF, molecular function.

complex of a PPI network or functional clustering module can help determine the unknown functions of proteins. In the present study, the MCODE (26) tool was applied to extract significant modules from the PPI network. The default parameters were set as Degree Cutoff: 2; Node Score Cutoff: 0.2; K-Core: 2; and Max. Depth: 100. Moreover, GO enrichment analysis was performed for genes in the selected modules with a threshold of a gene count  $>2$  and a P-value  $<0.05$ .

## Results

**RNA-seq analysis of the bacterial samples.** After read cleaning, there were 8088448, 7929058, 8070351, 8229630, 8240862, and 8193913 read pairs in MYQT1, MYQT2,

MYQT3, MYQT4, MYQT5, and MYQT6, respectively. The overall alignment rates to the closest reference genome were 72, 81, 93, 77, 82, and 82% for MYQT1, MYQT2, MYQT3, MYQT4, MYQT5, and MYQT6, respectively. In the IGV screenshot (Fig. 1A), we present the locus tags from SMDB11\_RS00620 to SMDB11\_RS00680. This genomic region was selected picked since most of the samples had a high read coverage. In the IGV plot, the vertical strips (in red, green, blue, or orange) indicate where the RNA-seq reads contained different nucleotides (mutated nucleotides/SNPs). The five samples excluding MYQT3 had similar SNP patterns, leading us to question whether the MYQT3 data corresponded to a different *S. marcescens* strain. As presented in Fig. 1B, each small scatter plot reveals the correlation of gene expression

Table I. Top 15 DEGs identified using three different calculation methods.

Gene_symbol	Degree	Gene_symbol	Betweenness	Gene_symbol	Closeness
SMDB11_RS17755	21	SMDB11_RS17755	5978.15	SMDB11_RS17755	0.028501127
SMDB11_RS00590	16	SMDB11_RS23335	2504.5398	SMDB11_RS04505	0.028292285
SMDB11_RS00615	15	SMDB11_RS04505	2078.2375	SMDB11_RS00590	0.028280772
SMDB11_RS00595	15	SMDB11_RS14800	2021.148	SMDB11_RS00595	0.028234817
SMDB11_RS04505	14	SMDB11_RS02765	1661.6104	SMDB11_RS14100	0.02822335
SMDB11_RS00620	14	SMDB11_RS16760	1243.2932	SMDB11_RS02545	0.028194726
SMDB11_RS00600	14	SMDB11_RS09335	1066.5082	SMDB11_RS16760	0.028114887
SMDB11_RS09335	13	SMDB11_RS23570	1013.2664	SMDB11_RS23335	0.028103517
SMDB11_RS00625	13	SMDB11_RS21855	1010	SMDB11_RS14910	0.028103517
SMDB11_RS02545	13	SMDB11_RS01845	915.4805	SMDB11_RS02550	0.028097836
SMDB11_RS14100	13	SMDB11_RS05590	890.28687	SMDB11_RS00615	0.028080808
SMDB11_RS14095	12	SMDB11_RS03340	874.0195	SMDB11_RS00620	0.028075136
SMDB11_RS22005	10	SMDB11_RS14915	855.25476	SMDB11_RS00600	0.028075136
SMDB11_RS22020	10	SMDB11_RS02545	767.4091	SMDB11_RS02555	0.028075136
SMDB11_RS14105	10	SMDB11_RS00590	710.21094	SMDB11_RS15030	0.028058134

DEGs, differentially expressed genes.

[presented and normalized transcripts per million (TPM)] between two samples. As revealed in the plot, MYQT3 had very a different expression pattern compared to MYQT1 and MYQT2, and thus, MYQT3 was excluded from the following analysis.

**Differential expression analysis.** edgeR calculates the quadratic mean-variance (dispersion) relationship to moderate the degree of dispersion across features (genes) (Fig. 2). With the threshold of  $\log_2 \text{FC} > 1$  and a P-value  $< 0.05$ , a total of 225 DEGs were identified. The most significant DEG was SMDB11\_RS09300 (GTP cyclohydrolase Fole2) with a  $\log_2 \text{FC}$  of 6.4. The heat map is presented in Fig. 1C.

Using IGV, we identified the genomic region where the most significant DE gene was located, which was the region from locus tag SMDB11\_RS00610 to SMDB11\_RS00625 (siroheme synthase, sulfate adenylyltransferase subunit 2, sulfate adenylyltransferase, and adenylyl-sulfate kinase) (Fig. 3A). The four genes were all identified as DEGs by edgeR, and the four genes were highly expressed in the MYQT1 and MYQT2 groups compared to that in the other groups (MYQT4, MYQT5, and MYQT6). The IGV plot of this region strongly supported the conclusion that the four genes belonged to the same operon. Additionally, the genomic region from locus tag SMDB11\_RS14095 to SMDB11\_RS14110 (sulfate/thiosulfate transporter subunit, sulfate/thiosulfate transporter permease subunit, sulfate/thiosulfate transporter subunit, and thiosulfate transporter subunit) (Fig. 3B) was also assessed. The four genes were all identified as DEGs by edgeR, and the four genes were highly expressed in the MYQT1 and MYQT2 groups compared to that in the other groups (MYQT4, MYQT5, and MYQT6). Once again, the IGV plot of this region strongly supported the conclusion that the four genes belonged to the same operon.

**Functional enrichment analysis of DEGs.** The 225 DEGs were used to perform functional enrichment analysis, and several GO terms related to antibiotic-resistant mechanisms were identified. The initial assessment of the two sets of significant DE genes and their gene names (in the two IGV plots) indicated that hydrogen sulfide metabolic process and sulfate transmembrane-transporting ATPase activity may be enriched. Specifically, as revealed in Fig. 4, the first two enriched functional groups were GO:0070814~hydrogen sulfide biosynthetic process and GO:1901682~sulfur compound transmembrane transporter activity. The first two GO terms mostly reflected the two sets of DEGs (operons) we identified in the DEG analysis. The other GO term related to antibiotics-resistant mechanisms was GO:0043190~ATP-binding cassette (ABC) transporter complex.

**Construction and analysis of the PPI network and extraction of significant modules.** The PPI network was constructed (Fig. 5A) and consisted of 140 nodes (proteins) and 318 edges (interactions). After analyzing three types of network topology properties of nodes in the PPI network, 15 important nodes were identified, as revealed in Table I. The results indicated that four DEGs (SMDB11\_RS17755, SMDB11\_RS00590, SMDB11\_RS04505, and SMDB11\_RS02545) belonged to the top 15 genes regardless of the calculation method used.

With the use of the MCODE plug-in, the two modules with the highest score were obtained (Fig. 5B and C). As revealed in Fig. 5B, cluster 1 (score=11.27) had 12 nodes and 62 interactions. Cluster 2 (score=8), as revealed in Fig. 4C, consisted of 9 nodes and 32 interactions. In special, SMDB11\_RS00590 and SMDB11\_RS04505 belonged to cluster 1. Moreover, enrichment analysis of the genes in the enriched clusters (Fig. 6) was performed. No GO terms were identified for genes in cluster 2, and there were 41 GO terms enriched for cluster 1, such as hydrogen sulfide metabolic

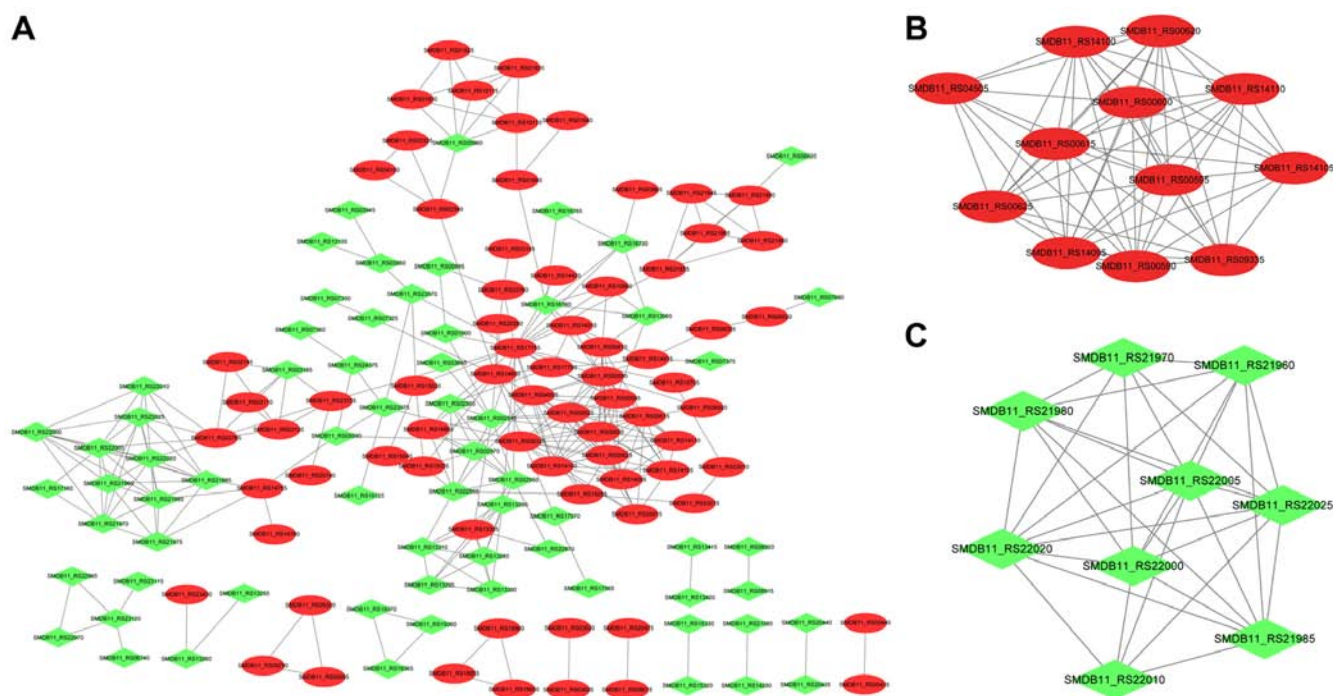


Figure 5. PPI network and two significant clusters. (A) PPI network. (B and C) Two significant clusters extracted from the PPI network. Red indicates upregulated genes, and green indicates downregulated genes. PPI, protein-protein interaction.

process, sulfate assimilation, and sulfur compound biosynthetic process.

## Discussion

Understanding the genetic mechanisms that underlie the antibiotic resistance of bacteria is a critical issue. In this study, we used RNA-seq to investigate the patterns of gene expression that may be associated with the antibiotic resistance mechanisms of *S. marcescens*. A total of 225 DEGs were identified, of which upregulated SMDB11\_RS09300 (GTP cyclohydrolase FolE2) was the most significant with a log<sub>2</sub> FC of 6.4, and these DEGs were enriched in different GO terms, including hydrogen sulfide biosynthetic process, sulfur compound transmembrane transporter activity, and ABC transporter complex. Additionally, several genes were identified to be important genes in the PPI network, including SMDB11\_RS17755 (upregulated; glutamate synthase large subunit), SMDB11\_RS00590 (upregulated; sulfite reductase subunit A), and SMDB11\_RS04505 (upregulated; cystathionine  $\beta$ -synthase). Functional enrichment analysis of genes in significant clusters revealed that genes were associated with sulfur metabolism.

SMDB11\_RS09300 encodes GTP cyclohydrolase FolE2 (27), an enzyme involved in the biosynthesis of folic acid and pteridines (28,29). There is evidence that the folic acid biosynthesis pathway may be a potential target for the development of antibiotics, and this has been validated by the clinical use of several drugs (30). Rengarajan *et al* demonstrated that folate metabolism was a target for resistance to a type of antibiotic (31). In the present study, upregulated SMDB11\_RS09300 was revealed to have the highest expression change in the multidrug-resistant *S. marcescens*, which was consistent with previous studies indicating that the upregulation of SMDB11\_RS09300 may play a significant

role in the multidrug-resistant mechanisms of *S. marcescens* by participating in folate metabolism.

Glutamate synthase is important as it provides glutamate for glutamine synthetase reaction (32). A study showed that the export of glutamine synthetase was associated with the formation of the poly-L-glutamate/glutamine cell wall structure of organisms (33). A decrease in extracellular glutamine synthetase activity can inhibit bacterial growth (34). Evidence has indicated that several cell-wall-related genes can be strongly expressed in *Staphylococcus aureus* in response to antibiotics, such as *gltD*, which encodes the small subunit of glutamate synthase (35). In the present study, it was revealed that SMDB11\_RS17755 (glutamate synthase large subunit) was upregulated and was a hub protein in the PPI network, suggesting that the upregulation of this gene may contribute to cell wall metabolism, which may defend *S. marcescens* against the antibacterial activities of the agents.

Moreover, SMDB11\_RS00590 (sulfite reductase subunit  $\alpha$ ) and SMDB11\_RS04505 (cystathionine  $\beta$ -synthase) were also upregulated and played important roles in the PPI network in this study. The sulfite reductases catalyze the reduction of sulfite to sulfide (36), and cystathionine  $\beta$ -synthase is also a sulfur metabolism enzyme (37). Synthetic antimicrobial agents such as the 'sulfa drugs' (sulfonamides) have also been brought into wider usage, and they can inhibit steps in folic acid metabolism (38). Sulfur metabolic pathways are essential for survival and virulence of many pathogenic bacteria and represent a promising new area for therapy against multidrug resistant microbes (39). In the present study, the identified 225 DEGs and genes in the significant cluster 1 were mainly associated with sulfur metabolism. Thus, it was concluded that the upregulation of SMDB11\_RS00590 and SMDB11\_RS04505, which were involved in the sulfur metabolism in *S. Marcescens*, may be critical in its antibiotic resistance

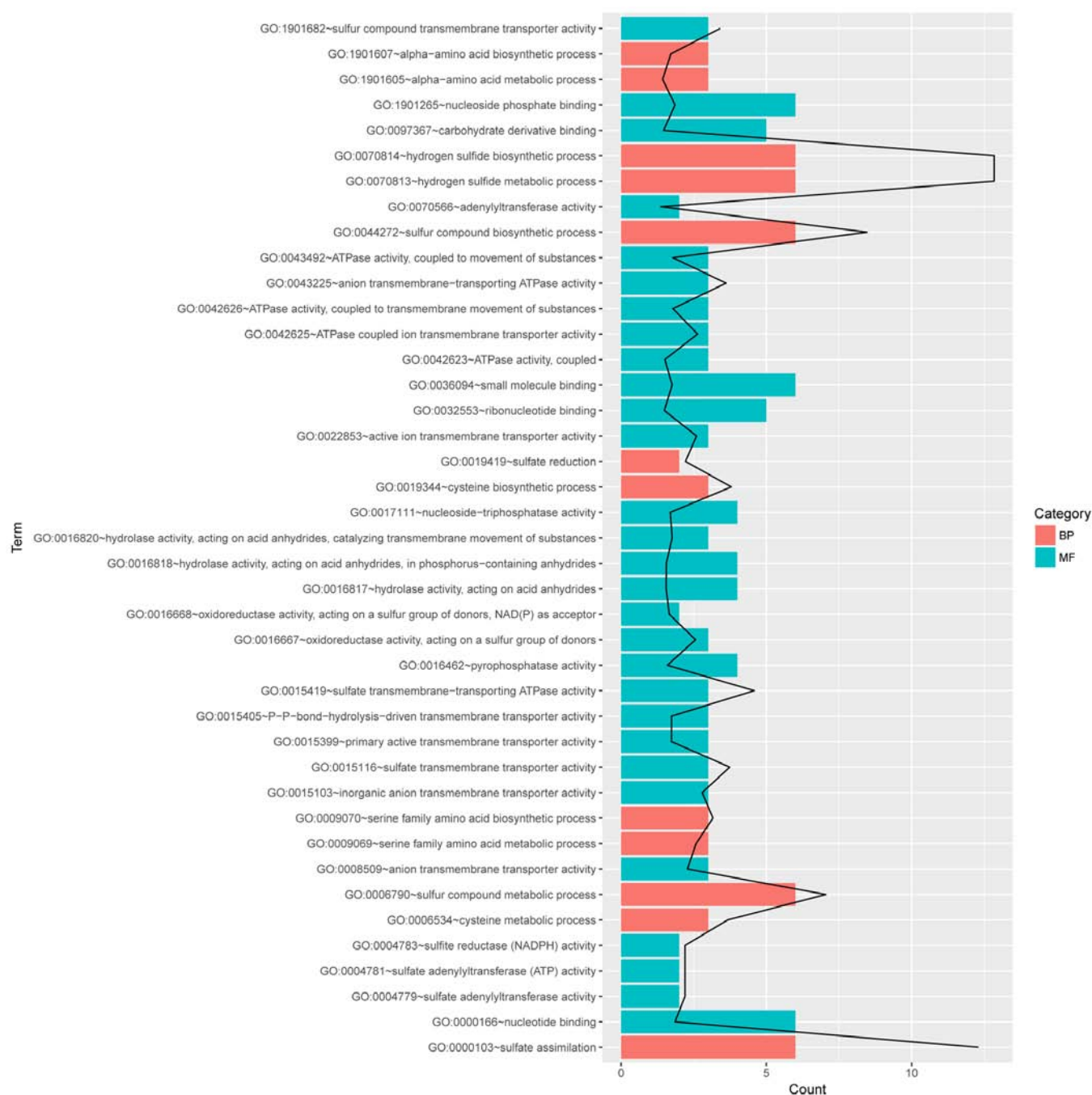


Figure 6. Functional enrichment analysis of genes in the two modules. The black line indicates the  $-\log_{10}(P\text{-value})$ . BP, biological process; MF, molecular function.

mechanisms. However, further studies are required to validate the roles of these genes.

However, the major limitation of this study was that a small number of replicates was used, which did not provide sufficient statistical power to assess the significance of the findings. Thus, the results of this study require confirmation in the future, i.e., when more replicates and confirmatory experiments using additional techniques (e.g., qPCR) are available. Another limitation of this study was that the associations used to construct the PPI network were derived from another species due to the lack of *S. marcescens* in the database. Thus, more studies are required to verify the biological interpretation of these results.

In conclusion, this study profiled genes in multi-drug-resistant *S. marcescens* using RNA sequencing. SMDB11\_RS09300 may play a significant role in the multi-drug-resistant mechanisms of *S. marcescens* by participating in folate metabolism. SMDB11\_RS17755 may contribute to the integrity of cell membranes, which is involved in the multi-drug resistance of *S. marcescens*. The upregulation of SMDB11\_RS00590 and SMDB11\_RS04505 in *S. marcescens* may be critical in its antibiotic resistance mechanisms. Further studies with a large panel of isolates are required to validate these findings. However, these findings are important and will aid in better understanding bacterial resistance to these drugs.



## Acknowledgements

Not applicable.

## Funding

The present study was supported by The Medical and Health Science and Technology Plan of Zhejiang Province (Program no. 2019KY134) and The Hangzhou Health and Family Planning Technology Plan (Program no. 2018Z07).

## Availability of data and materials

The datasets used and/or analyzed during the current study are available from the corresponding author on reasonable request.

## Authors' contributions

ZL and MD conceived the present study. ZL drafted the manuscript. MX and HW collected and analyzed the data. LW interpreted the data. All authors read and approved the final manuscript, and agreed to be accountable for all aspects of the work in ensuring that questions related to the accuracy or integrity of any part of the work are appropriately investigated and resolved.

## Ethics approval and consent to participate

Not applicable.

## Patient consent for publication

Not applicable.

## Competing interests

The authors declare that they have no competing interests.

## References

- Courtney CM, Goodman SM, McDaniel JA, Madinger NE, Chatterjee A and Nagpal P: Photoexcited quantum dots for killing multidrug-resistant bacteria. *Nat Mater* 15: 529-534, 2016.
- Iguchi A, Nagaya Y, Pradel E, Ooka T, Ogura Y, Katsura K, Kurokawa K, Oshima K, Hattori M, Parkhill J, *et al*: Genome evolution and plasticity of *Serratia marcescens*, an important multidrug-resistant nosocomial pathogen. *Genome Biol Evol* 6: 2096-2110, 2014.
- Blair JM, Webber MA, Baylay AJ, Ogbolu DO and Piddock LJ: Molecular mechanisms of antibiotic resistance. *Nat Rev Microbiol* 13: 42-51, 2015.
- Alekshun MN and Levy SB: Molecular mechanisms of antibacterial multidrug resistance. *Cell* 128: 1037-1050, 2007.
- Ma XJ, Yang HF, Liu YY, Mei Q, Ye Y, Li HR, Cheng J and Li JB: The emergence of the 16S rRNA methyltransferase RmtB in a multidrug-resistant *Serratia marcescens* isolate in China. *Ann Lab Med* 35: 172-174, 2015.
- Su W, Zhu Y, Deng N and Li L: Imipenem-resistance in *Serratia marcescens* is mediated by plasmid expression of KPC-2. *Eur Rev Med Pharmacol Sci* 21: 1690-1694, 2017.
- Olaitan AO, Morand S and Rolain JM: Mechanisms of polymyxin resistance: Acquired and intrinsic resistance in bacteria. *Front Microbiol* 5: 643, 2014.
- Rabbani B, Nakaoka H, Akhondzadeh S, Tekin M and Mahdih N: Next generation sequencing: Implications in personalized medicine and pharmacogenomics. *Mol Biosyst* 12: 1818-1830, 2016.
- Crofts TS, Gasparrini AJ and Dantas G: Next-generation approaches to understand and combat the antibiotic resistance. *Nat Rev Microbiol* 15: 422-434, 2017.
- Crowley E, Bird P, Fisher K, Goetz K, Boyle M, Benzinger MJ Jr, Juenger M, Agin J, Goins D and Johnson R: Evaluation of the VITEK 2 Gram-negative (GN) microbial identification test card: Collaborative study. *J AOAC Int* 95: 778-785, 2012.
- McClure R, Balasubramanian D, Sun Y, Bobrovskyy M, Sumby P, Genco CA, Vanderpool CK and Tjaden B: Computational analysis of bacterial RNA-Seq data. *Nucleic Acids Res* 41: e140, 2013.
- Bolger AM, Lohse M and Usadel B: Trimmomatic: A flexible trimmer for Illumina sequence data. *Bioinformatics* 30: 2114-2120, 2014.
- Langmead B and Salzberg SL: Fast gapped-read alignment with Bowtie 2. *Nat Methods* 9: 357-359, 2012.
- Robinson JT, Thorvaldsdóttir H, Winckler W, Guttman M, Lander ES, Getz G and Mesirov JP: Integrative genomics viewer. *Nat Biotechnol* 29: 24-26, 2011.
- Quinlan AR and Hall IM: BEDTools: A flexible suite of utilities for comparing genomic features. *Bioinformatics* 26: 841-842, 2010.
- Robinson MD and Oshlack A: A scaling normalization method for differential expression analysis of RNA-seq data. *Genome Biol* 11: R25, 2010.
- Huang da W, Sherman BT and Lempicki RA: Systematic and integrative analysis of large gene lists using DAVID bioinformatics resources. *Nat Protoc* 4: 44-57, 2009.
- Gene Ontology Consortium: Gene ontology consortium: Going forward. *Nucleic Acids Res* 43 (Database Issue): D1049-D1056, 2015.
- Szklarczyk D, Franceschini A, Wyder S, Forslund K, Heller D, Huerta-Cepas J, Simonovic M, Roth A, Santos A, Tsafou KP, *et al*: STRING v10: Protein-protein interaction networks, integrated over the tree of life. *Nucleic Acids Res* 43 (Database Issue): D447-D452, 2015.
- Shannon P, Markiel A, Ozier O, Baliga NS, Wang JT, Ramage D, Amin N, Schwikowski B and Ideker T: Cytoscape: A software environment for integrated models of biomolecular interaction networks. *Genome Res* 13: 2498-2504, 2003.
- Opsahl T, Agneessens F and Skvoretz J: Node centrality in weighted networks: Generalizing degree and shortest paths. *Soc Netw* 32: 245-251, 2010.
- Cukierski WJ and Foran DJ: Using betweenness centrality to identify manifold shortcuts. *Proc IEEE Int Conf Data Min* 2008: 949-958, 2008.
- Du Y, Gao C, Chen X, Hu Y, Sadiq R and Deng Y: A new closeness centrality measure via effective distance in complex networks. *Chaos* 25: 033112, 2015.
- Tang Y, Li M, Wang J, Pan Y and Wu FX: CytoNCA: A cytoscape plugin for centrality analysis and evaluation of protein interaction networks. *Biosystems* 127: 67-72, 2015.
- Safari-Alighiarloo N, Taghizadeh M, Rezaei-Tavirani M, Golizadeh B and Peyvandi AA: Protein-protein interaction networks (PPI) and complex diseases. *Gastroenterol Hepatol Bed Bench* 7: 17-31, 2014.
- Bader GD and Hogue CW: An automated method for finding molecular complexes in large protein interaction networks. *BMC Bioinformatics* 4: 2, 2003.
- Sankaran B, Bonnett SA, Shah K, Gabriel S, Reddy R, Schimmel P, Rodionov DA, de Crécy-Lagard V, Hermann JD, Iwata-Reuyl D and Swairjo MA: Zinc-independent folate biosynthesis: Genetic, biochemical, and structural investigations reveal new metal dependence for GTP cyclohydrolase IB. *J Bacteriol* 191: 6936-6949, 2009.
- Rebelo J, Auerbach G, Bader G, Bracher A, Nar H, Hösl C, Schramek N, Kaiser J, Bacher A, Huber R and Fischer M: Biosynthesis of pteridines. Reaction mechanism of GTP cyclohydrolase I. *J Mol Biol* 326: 503-516, 2003.
- Babitzke P, Gollnick P and Yanofsky C: The *mtrAB* operon of *Bacillus subtilis* encodes GTP cyclohydrolase I (MtrA), an enzyme involved in folic acid biosynthesis, and MtrB, a regulator of tryptophan biosynthesis. *J Bacteriol* 174: 2059-2064, 1992.
- Birmingham A and Derrick JP: The folic acid biosynthesis pathway in bacteria: Evaluation of potential for antibacterial drug discovery. *Bioessays* 24: 637-648, 2002.
- Rengarajan J, Sassetti CM, Naroditskaya V, Sloutsky A, Bloom BR and Rubin EJ: The folate pathway is a target for resistance to the drug para-aminosalicylic acid (PAS) in mycobacteria. *Mol Microbiol* 53: 275-282, 2004.

32. Pan FL and Coote JG: Glutamine synthetase and glutamate synthase activities during growth and sporulation in *Bacillus subtilis*. *J Gen Microbiol* 112: 373-377, 1979.
33. Harth G, Zamecnik PC, Tang JY, Tabatadze D and Horwitz MA: Treatment of *Mycobacterium tuberculosis* with antisense oligonucleotides to glutamine synthetase mRNA inhibits glutamine synthetase activity, formation of the poly-L-glutamate/glutamine cell wall structure, and bacterial replication. *Proc Natl Acad Sci USA* 97: 418-423, 2000.
34. Harth G and Horwitz MA: An inhibitor of exported *Mycobacterium tuberculosis* glutamine synthetase selectively blocks the growth of pathogenic mycobacteria in axenic culture and in human monocytes: Extracellular proteins as potential novel drug targets. *J Exp Med* 189: 1425-1436, 1999.
35. Utaida S, Dunman PM, Macapagal D, Murphy E, Projan SJ, Singh VK, Jayaswal RK and Wilkinson BJ: Genome-wide transcriptional profiling of the response of *Staphylococcus aureus* to cell-wall-active antibiotics reveals a cell-wall-stress stimulon. *Microbiology* 149: 2719-2732, 2003.
36. Schnell R, Sandalova T, Hellman U, Lindqvist Y and Schneider G: Siroheme- and [Fe4-S4]-dependent NirA from *Mycobacterium tuberculosis* is a sulfite reductase with a covalent Cys-Tyr bond in the active site. *J Biol Chem* 280: 27319-27328, 2005.
37. Bhattacharyya S, Saha S, Giri K, Lanza IR, Nair KS, Jennings NB, Rodriguez-Aguayo C, Lopez-Berestein G, Basal E, Weaver AL, *et al*: Cystathionine beta-synthase (CBS) contributes to advanced ovarian cancer progression and drug resistance. *PLoS One* 8: e79167, 2013.
38. Bisht R, Katiyar A, Singh R and Mittal P: Antibiotic resistance-A global issue of concern. *Asian J Pharm Clin Res* 2: 34-39, 2009.
39. Bhawe DP, Muse WB III and Carroll KS: Drug targets in mycobacterial sulfur metabolism. *Infect Disord Drug Targets* 7: 140-158, 2007.



This work is licensed under a Creative Commons Attribution-NonCommercial-NoDerivatives 4.0 International (CC BY-NC-ND 4.0) License.